W. Dorn · K. Dethloff · A. Rinke · E. Roeckner

Competition of NAO regime changes and increasing greenhouse gases and aerosols with respect to Arctic climate projections

Abstract Regional magnitudes and patterns of Arctic winter climate changes in consequence of regime changes of the North Atlantic Oscillation (NAO) are analyzed using a regional atmospheric climate model. The regional model has been driven with data of positive and negative NAO phases from a control simulation as well as from a time-dependent greenhouse gas and aerosol scenario simulation. Both global model simulations include a quite realistic interannual variability of the NAO with pronounced decadal regime changes and no or rather weak long-term NAO trends. The results indicate that the effects of NAO regime changes on Arctic winter temperatures and precipitation are regionally significant over most of northwestern Eurasia and parts of Greenland. In this regard, mean winter temperature variations of up to 6 K may occur over northern Europe. Precipitation and synoptic variability are also regionally modified by NAO regime changes, but not as significantly as temperatures. However, the climate changes associated with the NAO are in some regions clearly stronger than those attributed to enhanced greenhouse gases and aerosols, indicating that projected global changes of the atmospheric composition and internal circulation changes are competing with each other in their importance for the Arctic climate evolution in the near future. The knowledge of the future NAO trend on decadal and longer time scales appears to be vitally important in terms of a regional assessment of climate scenarios for the Arctic.

W. Dorn (✉) · K. Dethloff · A. Rinke
Alfred Wegener Institute for Polar and Marine Research,
Telegrafenberg A43, 14473 Potsdam, Germany
E-mail: wdorn@awi-potsdam.de

E. Roeckner
Max Planck Institute for Meteorology,
Bundesstraße 55, 20146 Hamburg, Germany

1 Introduction

Scenario simulations of global climate models consistently predict the worldwide strongest warming over the northern polar region as a result of increasing greenhouse gases (e.g. Haywood et al. 1997; Stouffer and Manabe 1999; Roeckner et al. 1999; Voss and Mikolajewicz 2001). These model studies highlight the Arctic as a region where global changes have extremely strong impacts, probably caused by a variety of feedback mechanisms, whereby the Arctic responds to global changes rapidly and more sensitively than any other region of the Earth. However, the results from different models as well as from different scenarios disagree regarding both the magnitude of the projected climate changes and the regional aspects of these changes (Cubasch et al. 2001), but a realistic projection of the future Arctic climate evolution is essential, because changes in the Arctic climate may have global consequences, for example increasing sea levels from melting of the cryosphere, slowing of the Atlantic thermohaline circulation due to reduced North Atlantic deep water formation, and increasing greenhouse gas levels due to amplified natural carbon dioxide and methane emissions in the Arctic.

In many cases, future changes of the Arctic climate are merely attributed to enhanced greenhouse gas levels, even though the similar existing effects of natural dynamical processes in the climate system have not been completely understood until now, because of the high complexity of the climate system due to the nonlinear interactions between its components. Internally caused climate fluctuations associated with nonlinear instability and feedback processes in the atmosphere itself and in the atmosphere–ocean system are important mechanisms for natural climate changes and have been discussed, e.g. by Hansen et al. (1997), Dethloff et al. (1998), Palmer (1999), and Handorf et al. (1999). In order to continue discussions on the future evolution of the Arctic climate,

the effects of natural climate variability and in particular their regional magnitude have to be taken into account.

One major phenomenon of natural climate variability in the Northern Hemisphere is the North Atlantic Oscillation (NAO) and the associated Arctic Oscillation (AO) which appear to be fundamentally the same physical phenomenon (Kerr 1999; Wallace 2000; Ambaum et al. 2001). The NAO refers to a meridional oscillation in atmospheric mass and is characterized by antipodal pressure anomalies in the areas of the Icelandic low and the Azores high (e.g. Hurrell and van Loon 1997). The NAO is most pronounced during winter and, due to the meridional pressure gradient changes over the North Atlantic, associated with changes in the westerlies, which transport warm and humid air across the Atlantic towards Europe. The recently observed warming over much of extra-tropical Eurasia during the winter half year is closely related to the high-index or positive phase of the NAO which occurs since the 1970s (Folland et al. 2001). Because of the spatially and temporally sparse observational data in polar latitudes, the influence of the NAO on the Arctic climate is not completely known.

Comparison studies of the performance of global climate models in polar latitudes have shown that different models produce large variations in the simulation of the Arctic climate (e.g. Chen et al. 1995; Tao et al. 1996). These discrepancies appear in consequence of inadequacies in the parameterization of physical processes and the fairly coarse horizontal resolution of global models (Curry et al. 1996; Rinke et al. 1997). A high-resolution regional climate model (RCM) is a powerful tool for improving the simulation of regional effects of the Arctic climate as a result of finer resolved orography and land–sea contrast, better resolved nonlinear interactions between the large-scale and smaller scales, improved simulations of hydrodynamic instability processes and synoptic cyclones, and improved description of hydrological and precipitation processes (e.g. Lynch et al. 1995; Giorgi and Marinucci 1996; Noguer et al. 1998; Rinke and Dethloff 2000).

In the present study, a dynamical downscaling of global climate model outputs has been performed with a high-resolution RCM for the Arctic atmosphere. By means of this approach, information about the large-scale atmospheric structures, e.g. concerning the NAO pattern, are transferred from the global model into the regional model, whereas internal Arctic climate processes can be simulated closer to reality using higher horizontal resolution. The primary object of this study was to obtain a realistic estimate of magnitudes and regional aspects of Arctic climate variations connected with NAO regime changes, particularly having regard to the projected changes of the atmospheric composition.

2 Regional climate model description

The Arctic climate simulations have been performed using the regional atmospheric climate model HIRHAM4 which was developed by Christensen et al. (1996) and adapted for simulations of the Arctic climate by Dethloff et al. (1996). The dynamics of HIRHAM4 are based on the limited-area model HIRLAM (Gustafsson 1993) and include prognostic equations for horizontal wind components, temperature, specific humidity, cloud water, and surface pressure. Additionally, diagnostic equations exist for vertical wind, geopotential, cloud cover, and mixed clouds.

Furthermore, HIRHAM4 uses the physical parameterization package of the general circulation model (GCM) ECHAM4 (Roeckner et al. 1996) with parameterizations for radiation, land surface processes, sea surface sea-ice processes, planetary boundary layer, gravity wave drag, cumulus convection, and large-scale condensation, including balance equations for energy and hydrology at the surface and a heat conductivity equation for the temperatures in five soil layers between the surface and 10 m depth. HIRHAM4 allows for 16 diverse soil types (each with or without snow cover), open ocean, sea-ice, and Greenland glacier, and uses prescribed parameters for soil and vegetation parameters.

The integration domain comprises the whole Arctic north of 65°N with 110 by 100 grid points in a horizontal resolution of 0.5° by 0.5°, corresponding to grid elements of approximately 50 km by 50 km. The vertical resolution is given by 19 irregularly spaced levels in hybrid sigma-pressure-coordinates from the surface up to 10 hPa with the highest resolution in the planetary boundary layer (approx. five levels). The model calculations have been carried out with a time step of 240 s.

3 Global climate model experiments

3.1 Model and experiment description

At the lateral and lower boundaries, the regional model has been driven with data from two various global climate model simulations: a long-term control simulation of the coupled atmosphere–ocean GCM ECHO-G (ECHAM4/HOPE-G) (Legutke and Voss 1999) and a greenhouse gas and aerosol scenario simulation of the coupled atmosphere–ocean GCM ECHAM4/OPYC3 (Roeckner et al. 1999). The ECHO-G model consists of the atmosphere GCM ECHAM4 (Roeckner et al. 1996) at T30/L19 resolution (horizontal grid point distance of approx. 3.75°; 19 vertical levels) and the global version of the Hamburg Ocean Primitive Equation GCM HOPE-G (Wolff et al. 1997), which incorporates a dynamic–thermodynamic sea-ice model with snow cover. A control simulation with ECHO-G has been carried out for 600 years with prescribed constant external forcing representative for the year 1990, especially with respect to greenhouse gases. Therefore, this simulation can only include climate variations caused by internal fluctuations within the atmosphere–ocean–ice system and can thus be used as a reference experiment for estimating the natural dimension of NAO related climate changes.

The ECHAM4/OPYC3 model likewise comprises the atmosphere GCM ECHAM4, but the selected simulation has been carried out at T42/L19 resolution (horizontal grid point distance of approx. 2.8°; 19 vertical levels) and with another ocean module, the OPYC3, which is a coupled sea-ice-mixed layer-isopycnal GCM (Oberhuber 1993a, b). A time-dependent forcing experiment has been carried out, which includes changes of the atmospheric concentrations of carbon dioxide, methane, nitrous oxide, and several industrial gases as well as sulfate aerosols (direct and indirect effect) and tropospheric ozone. The annual concentrations of these atmospheric components have been derived from observations for the years from 1860 to 1990 and from the anthropogenic emission scenario IS92a (Houghton et al. 1992) for the years from 1990 to 2050. For a more detailed description of the model and the design of the experiment see Roeckner et al. (1999). Using all these means, climate variations in this scenario simulation can thus be induced by both internal fluctuations within the atmosphere–ocean–ice system and changes of the atmospheric composition.

3.2 NAO variability

For identification of positive and negative phases of the NAO, a simple index has been used. According to Hurrell (1995), this NAO index has been calculated as the difference between the normalized mean winter (December–March) sea level pressure (SLP) anomalies at Lisbon, Portugal, and Stykkisholmur, Iceland. For the observational data shown, the SLP anomalies at each station were normalized relatively to the 120-year period 1864–1983. An analogous definition has been used to define the NAO index from both global model simulations, whereas the normalization at corresponding model grid points has been performed using the whole length of the respective simulation.

The time series of the observed and both simulated NAO indices are presented in Fig. 1. In accordance with the observed NAO index, both simulations show strong variations of the NAO index on annual and decadal time scales. The range of these variations is in the same order of magnitude, but extremely high values as observed in the early 1990s are infrequent in both simulations. Nevertheless, both simulations are able to produce a fairly realistic variability of the NAO with several high- and low-index phases. However, it seems that the intensity and frequency of the NAO has changed slightly during the last years of the scenario simulation. This is supported by the study of Corti et al. (1999), who have pointed out that anthropogenic forcing may project onto modes of natural climate variability in terms of a modulation of their frequency or intensity.
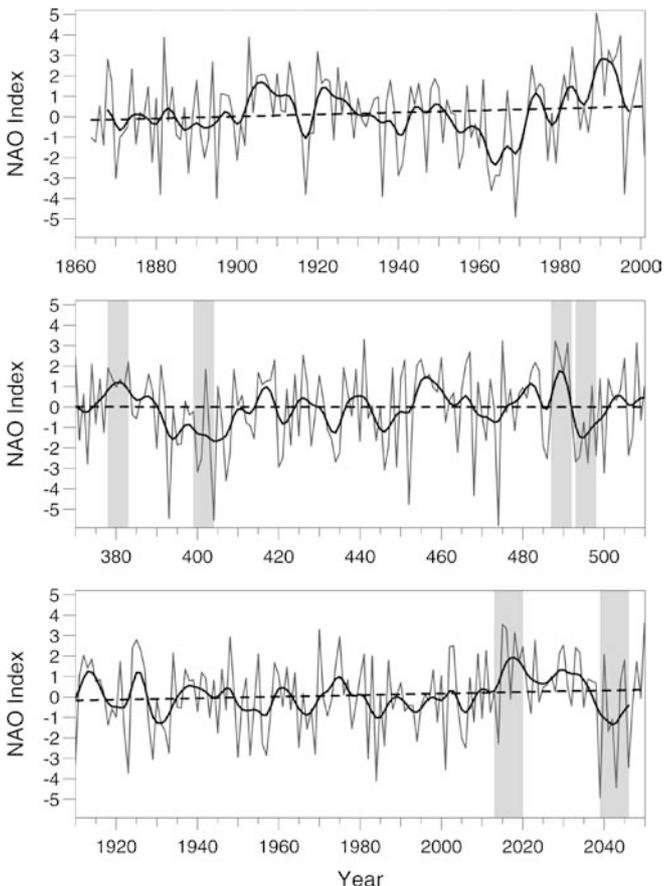
Nevertheless, it is particularly mentionable that in contrast to some other model studies (e.g. Ulbrich and Christoph 1999; Paeth et al. 1999), the scenario simulation does not show a significant trend of the NAO index. After a period of predominantly positive NAO from the 2010s to the 2030s, the NAO reenters its negative phase during the 2040s. This pronounced recurrence of a negative phase at the end of the simulation also appears in the non-local AO index as shown in Fig. 2. Following Thompson and Wallace (1998), the AO index is here defined as the principal component time series of the leading empirical orthogonal function (EOF) of wintertime (December–March) monthly mean SLP poleward of 20°N. Although the AO index shows a high correlation with the NAO index, both in the control simulation (correlation coefficient of 0.75) and in the scenario simulation (correlation coefficient of 0.73), the AO index of the scenario simulation features a statistically significant upward trend at the 95% confidence level. However, high- and low-index phases of the AO are largely identical as those of the NAO, in fact in both global model simulations.

3.3 Temperature trends

In consequence of increasing greenhouse gases and aerosols, the annual global mean surface air temperature in the scenario simulation rises due to an enhanced radiative forcing (see Roeckner et al. 1999). However, the temperature changes are reduced as compared to a scenario simulation without involvement of sulfate aerosols, especially at high northern latitudes. Nevertheless, the strongest warming appears in the northern polar region during winter. The time series of the mean 2 m air temperatures in winter (December to March) averaged over the region north of 60°N is presented in Fig. 3. Apart from pronounced annual and decadal variations of up to 4 K, the mean Arctic winter temperatures are nearly constant during the first part of the scenario simulation (approximately until 1980). The slight upward trend is statistically not significant. On the other hand, the second part of the scenario simulation is characterized by a pronounced upward trend which is statistically significant at the 99.9% confidence level. The mean Arctic warming from the 1970s to the 2040s is of about 5 K during winter (and less than 2 K during summer; not shown).

Fig. 1 Time series of the NAO index for winter (December–March) from observational data (*top*), from a segment of the control simulation (*middle*), and from the last years of the scenario simulation (*bottom*). The *thick solid lines* represent the 10-year low-pass-filtered time series, and the *dashed lines* represent the linear trends. Each *light gray bar* marks one of the selected periods for the regionalization of the Arctic climate

Fig. 2 Time series of the AO index for winter (December–March) from a segment of the control simulation (*top*), and from the last years of the scenario simulation (*bottom*). The *thick solid lines* represent the 10-year low-pass-filtered time series, and the *dashed lines* represent the linear trends. Each *light gray bar* marks one of the selected periods for the regionalization of the Arctic climate
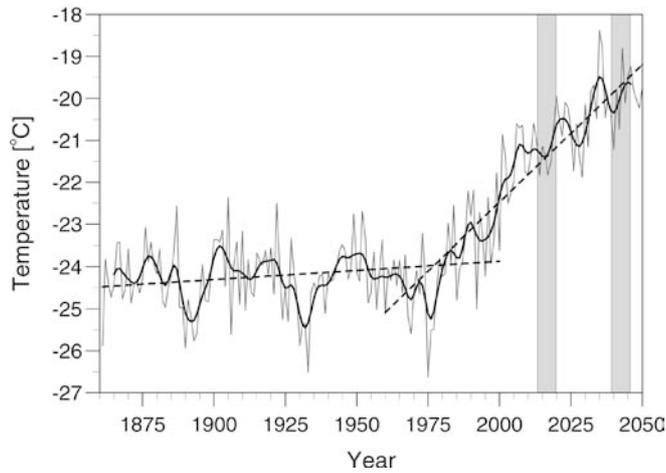
Fig. 3 Time series of mean 2 m air temperature in winter (December–March) averaged over the region north of 60°N from the scenario simulation. The *thick solid line* represents the 10-year low-pass-filtered time series, and the *dashed lines* represent the linear trends from 1860 to 2000 and from 1960 to 2050. Each *light gray bar* marks one of the selected periods for the regionalization of the Arctic climate

In contrast to the scenario simulation, there is naturally no statistically significant Arctic temperature trend throughout the control simulation. Moreover, there is also no correlation between the mean Arctic winter temperatures and the NAO index, either in the control simulation (correlation coefficient of –0.05) or in the scenario simulation (correlation coefficient of 0.02). Dorn et al. (2000) have shown that broadly warm and cold Arctic winter climate conditions are connected with two distinct circulation states of the Arctic atmosphere which differ clearly from the NAO. Nevertheless, significant local and regional Arctic temperature variations due to NAO regime changes cannot be excluded.

3.4 Selected periods for regionalization

Hurrell and van Loon (1997) have shown that the power spectrum of the observed NAO index has a maximum at 6 to 10-year periods. For this reason, several high- and low-index periods of this range have been selected for the dynamical downscaling of the Arctic climate. Four 6-year periods from the ECHO-G control simulation have been selected, from which two represent the positive and two the negative phase of the NAO. From the ECHAM4/OPYC3 scenario simulation only two periods have been selected, but each includes 8 years in order to enlarge the ensemble size. The limitation of one high-index and one low-index scenario period was necessary, because several equivalent periods do not occur due to the permanently increasing level of greenhouse gases. For demonstration, all selected periods are represented in Figs. 1 to 3 by light gray bars.

In addition, both positive and both negative phases from the control simulation have been summarized and labeled as CTRL+ or CTRL–, respectively. According to this, CTRL+ and CTRL– represent an ensemble of 12 winters with predominantly high or predominantly low NAO index. The difference of mean SLP between CTRL+ and CTRL– is shown in Fig. 4a. Compared to low NAO winters, high NAO winters are characterized by anomalously low pressure across the Arctic and high pressure over mid-latitudes, particularly over the Atlantic and southern Europe. This simulated NAO pattern corresponds largely with the NAO pattern from observations (see Hurrell 1995, Fig. 1), even though the Atlantic centres of action are located more to the east. However, it can be concluded that the control simulation reproduces the NAO pattern quite realistically.
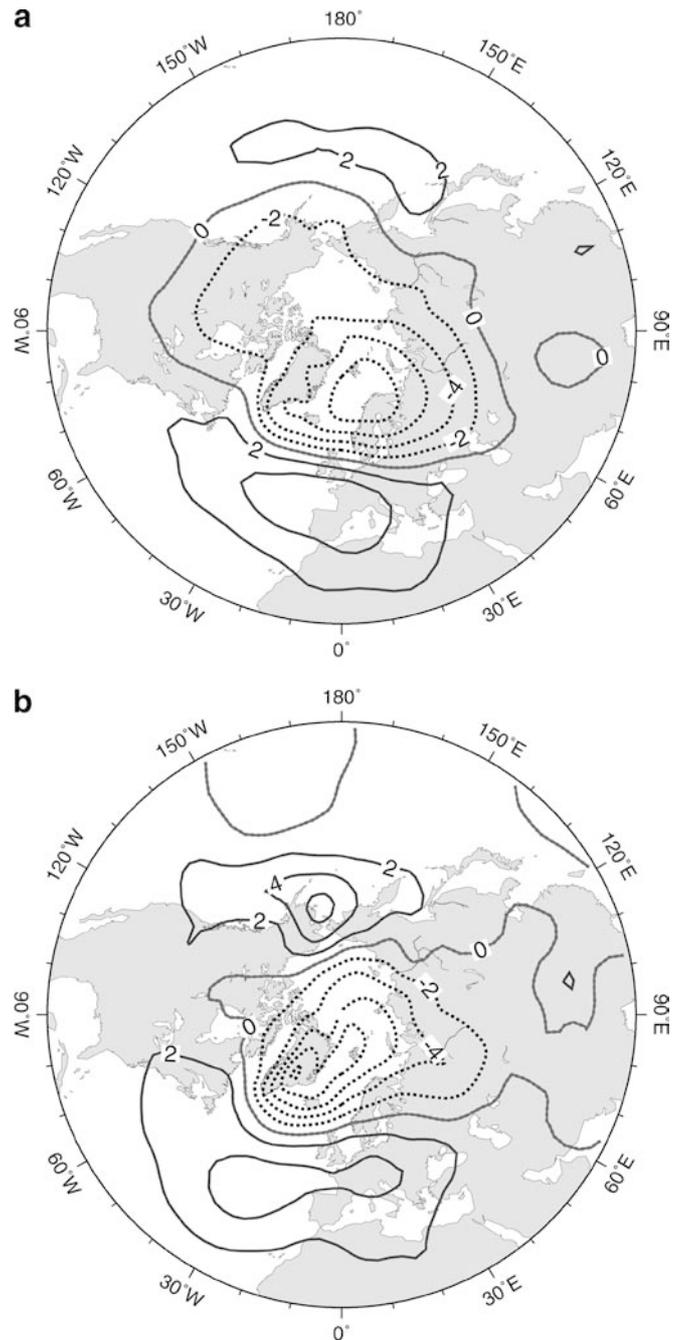
Fig. 4 Difference fields of mean sea level pressure (hPa) in winter (December–March) north of 20°N. **a** CTRL+ minus CTRL–; **b** SCEN+ minus SCEN–. *Positive* differences are represented by *solid contours* and *negative* differences are represented by *dashed contours*. The contour interval is 2 hPa

A similar pattern is also obtained by comparing the mean SLP of the two selected periods from the scenario simulation. Figure 4b shows the pressure difference between the scenario years 2013–2020 and 2039–2046. The first selected period is already characterized by a mean Arctic warming, but also by a high NAO index. Hence this period is labeled as SCEN+. In addition to broadly further increased mean winter temperatures in the years 2039–2046, the NAO is in its negative phase during this second selected period, and therefore the period is labeled as SCEN–.

In spite of the mean temperature changes as a result of increasing greenhouse gases and aerosols, the typical pressure differences between positive and negative NAO phases occur at least over the Atlantic sector of the Northern Hemisphere. Nevertheless, the Atlantic centres of action are slightly shifted in a westward direction in comparison with the control simulation, but they even bear a greater resemblance to the observed NAO pattern. However, a systematic northeastward shift of the NAO pattern, as found by Ulbrich and Christoph (1999) in a greenhouse gas only experiment with the same model, is not visible here. Indeed, there are much larger deviations in the NAO patterns over the North Pacific where the scenario simulation shows an amplification and northward shift of the positive pressure anomaly. This Pacific anomaly is normally clearly weaker than its Atlantic counterpart and located more to the south at mid-latitudes. A possible explanation is the massive reduction of winter sea-ice over the Bering Sea in the course of the scenario simulation (not shown), whereby the strength of the Aleutian low could increase by an enhanced surface heating (see Agnew 1993).

The pressure decrease in the area of the Aleutian low is consistent with a general decrease of SLP over the whole Arctic (see Roeckner et al. 1999), but the regional pressure variations associated with the NAO are much larger than the downward trend over most of the Arctic. The continuously changing atmospheric composition in the scenario simulation used seems to affect mean SLP within the Arctic, but it apparently changes the internal variability of the NAO and its typical pattern only inconsiderably, at least over the Atlantic sector.

4 Regional simulation results

Regional details of NAO related differences in Arctic temperatures, precipitation, and synoptic SLP variability are presented in this section. These results are based on simulations of the RCM HIRHAM4 driven by the selected periods of the control or scenario simulation, respectively, as described. For comparison, the corresponding results of the driving GCM simulations are discussed as well.

4.1 Temperature signal

Figure 5 shows the difference fields of the mean 2 m air temperature in winter between positive and negative NAO phases for the Arctic region. The natural temperature signal of the NAO is presented in Fig. 5a (HIRHAM4 simulations driven by the control simulation). The NAO impact is largest over the northwestern Eurasian continent with up to 6 K higher temperatures in CTRL+ than in CTRL−. These temperature differences are statistically significant at the 95% confidence level (derived from a two-sided Student's *t*-test applied to each individual grid point). In addition, higher temperatures of about 2 K appear during the positive phase in the vicinity of Svalbard and Novaya Zemlya. Simultaneously, lower temperatures of up to 5 K occur over Greenland and the Labrador Sea as well as with lower magnitudes in the areas of Iceland, eastern Siberia, and western Alaska. These negative temperature differences are also partly statistically significant, primarily over Greenland. Moreover, in the central Arctic, especially over

the Arctic Ocean, the natural temperature signal of the NAO is broadly weaker than in the marginal areas of the Arctic and is likely to be negligible.

In general, the influence of the NAO on Arctic temperatures is directly opposed in the western and eastern Arctic and stronger over land areas than over sea or sea-ice. Furthermore, the NAO effects appear much stronger over the Atlantic sector than over the Pacific sector of the Arctic and are most significant over Greenland and the northwestern Eurasian continent. Over northern Europe in particular, the simulated temperature signal of the NAO exceeds the observed warming over the past twenty years (see, e.g., Hurrell and van Loon 1997; Folland et al. 2001). Nevertheless, the simulated difference pattern bears a great resemblance to the observed temperature change pattern. Considering that the past two decades are characterized by both a shift to the positive NAO phase and increasing greenhouse gases, whereby at each case northern European temperatures are expected to rise, the simulation results suggest that the temperatures in this region are likely to respond to NAO regime changes much stronger than presumed in view of the observed warming.

The combined effects of the NAO and increasing greenhouse gases and aerosols on Arctic temperatures are shown in Fig. 5b (HIRHAM4 simulations driven by the scenario simulation). Despite the fact that the mean Arctic winter temperatures are approximately 1.3 K higher in SCEN− (2039–2046, see Fig. 3), there are not only negative (warming) but also positive (cooling) temperature differences between both periods. Subsequent to the positive phase, a strong warming of more than 6 K occurs over some areas of Alaska, the Labrador Sea, and Baffin Island, whereas a similar strong cooling only appears over the northern Barents Sea. Both the negative and the positive temperature differences are statistically significant at the 95% confidence level. The strong cooling over the northern Barents Sea is largely caused by a strong reduction of sea-ice in this area before and during the period with high NAO index. After the positive phase, the sea-ice cover in the Barents Sea is partly returning to pre-high-index conditions, whereas a strong decrease of sea-ice occurs over the Davis and Bering straits (not shown). As a reason for this phenomenon, a possible feedback between the NAO and increasing greenhouse gases cannot be excluded.

Nevertheless, a minor cooling until the years 2039 to 2046 also appears over the northwestern Eurasian continent, whereby this region particularly shows a very sensitive response to the NAO. Furthermore, the temperature dichotomy of the Arctic concerning the NAO impacts is not only in evidence under constant external forcing conditions, but also in a world with continuously changing climatic boundary conditions. Compared to the natural differences, the temperature effect of the NAO is superposed by a general temperature increase as a result of enhanced greenhouse gas and aerosol levels, and is nevertheless crucial for the regional temperature
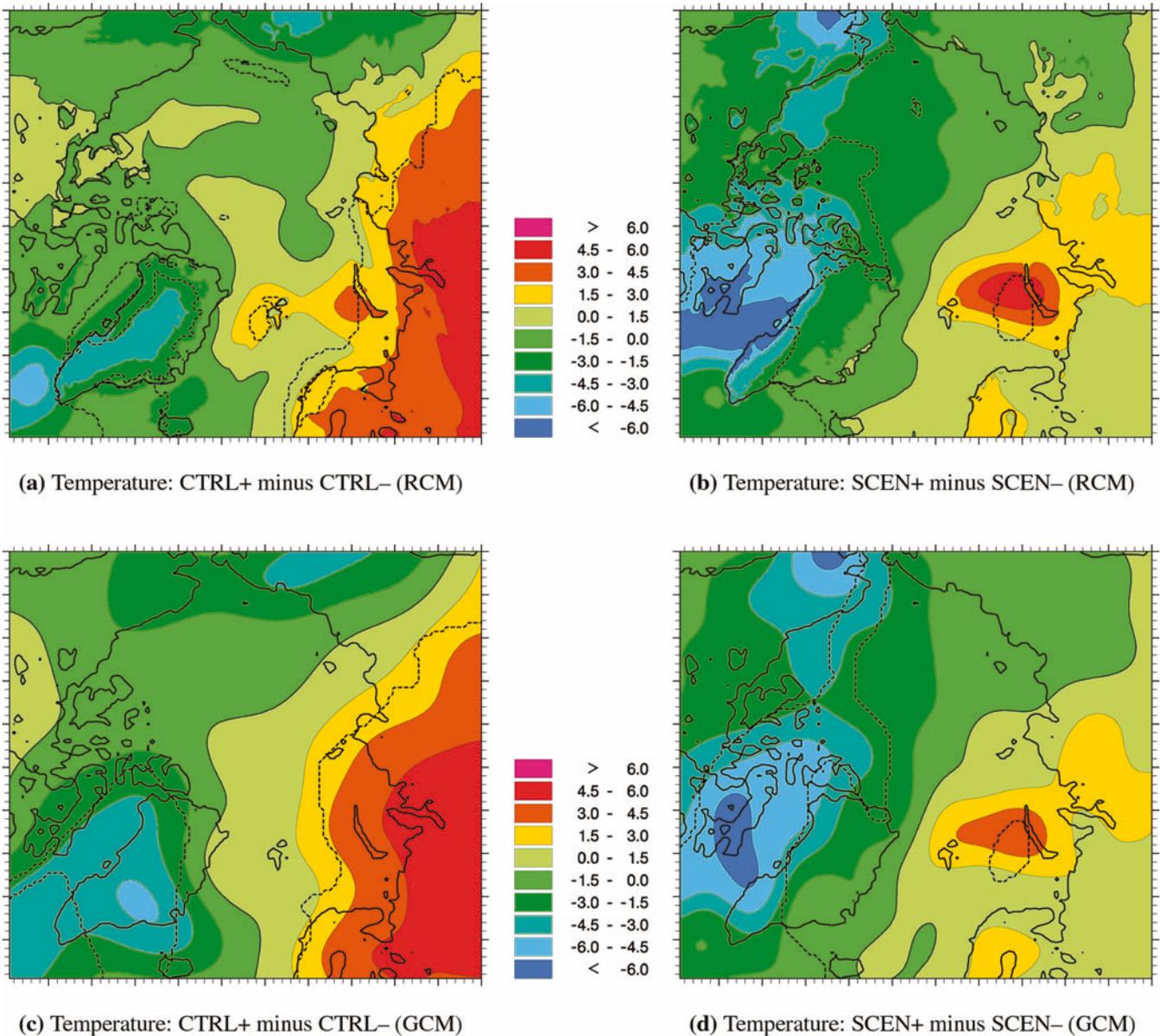
Fig. 5 Difference fields of mean 2 m air temperature (°C) in winter (December–March) for the Arctic region from simulations of the RCM HIRHAM4 (**a** CTRL+ minus CTRL–; **b** SCEN+ minus SCEN–), and the simulations of the driving GCMs (**c** CTRL+ minus CTRL–; **d** SCEN+ minus SCEN–). Coasts are represented by *solid contours*, and *dashed contours* represent the lower limit for 95% significance

evolution in the Arctic. Thus, NAO regime changes and increasing greenhouse gases and aerosols are clearly competing with each other.

These results also arise from analyzing the GCM simulations as shown in Fig. 5c, d. Although the difference patterns are predominantly identical to those of the RCM, there are deviations of about 2 K in some regions, especially in the vicinity of the Davis Strait and over the Barents and Kara seas. However the areas of statistically significant differences are quite similar. Because the 2 m air temperatures of the RCM are strongly influenced by sea surface temperatures and sea-ice cover from the GCM simulations used as lower boundary conditions, the RCM cannot diverge clearly

from the GCM over wide areas, and the benefit of the dynamical downscaling is here rather low.

4.2 Precipitation signal

The difference fields of the mean winter precipitation between positive and negative NAO phases are shown in Fig. 6. The natural precipitation signal of the NAO is presented in Fig. 6a (HIRHAM4 simulations driven by the control simulation). In broad agreement with observations (e.g. Hurrell 1995; Bromwich et al. 1999), more precipitation occurs over the eastern North Atlantic and northwestern Eurasia during the positive

(a) Precipitation: CTRL+ minus CTRL– (RCM)

(b) Precipitation: SCEN+ minus SCEN– (RCM)

(c) Precipitation: CTRL+ minus CTRL– (GCM)

(d) Precipitation: SCEN+ minus SCEN– (GCM)
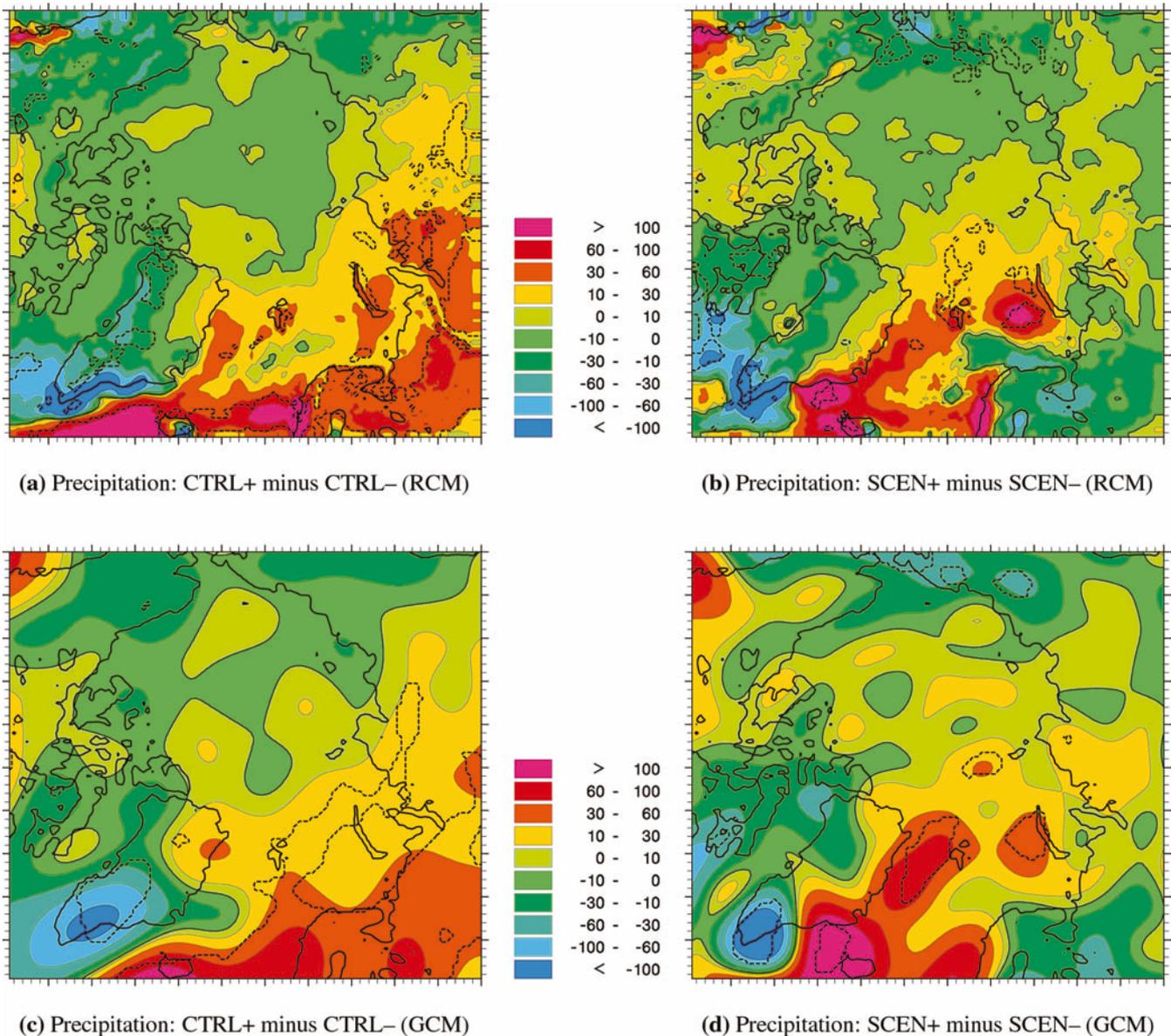
Fig. 6a–d As in Fig. 5 but for mean winter precipitation (mm)

NAO phase, whereas the negative phase is characterized by higher precipitation amounts over the Labrador Sea and over southern and western Greenland. These differences are not statistically significant everywhere at the 95% confidence level but only in some regions where the precipitation difference is extremely high or where the total precipitation amounts are relatively low.

In contrast to the temperature differences, the difference field of precipitation shows many more regional details which are particularly dependent on the orography, for example at the orographically strongly structured Pacific coast of North America. However, the precipitation differences also bear some resemblance to the temperature differences, especially the Arctic dichotomy mentioned concerning the NAO, which appears to have higher values over the eastern Arctic and lower values over the western Arctic during the positive

NAO phase. In addition, the precipitation differences over the central Arctic are low and statistically not significant, and the effects of the NAO on the precipitation are larger over the Atlantic sector of the Arctic than over the Pacific sector.

Very strong regional distinctions in the precipitation signal appear over Greenland. However, despite some more than 100 mm higher precipitation amounts on the southern and western coasts of Greenland during the negative NAO phase, statistically significant differences occur only over some parts of the Greenland ice sheet where the total precipitation is very low. Furthermore, the precipitation on the northeastern coast of Greenland is even higher during the positive phase, resulting in directly opposed precipitation signals on the western and eastern sides of northern Greenland. This simulation result is in qualitatively high agreement with the studies

by Appenzeller et al. (1998) and Bromwich et al. (1999). However, it was found that the correlation coefficients between the precipitation at single grid points of Greenland and the NAO index never exceed an absolute value of 0.35. Thus it appears that the simulated inter-annual variability of precipitation is very high, whereby the winter precipitation over most of Greenland is more strongly influenced by interannual variability than by the NAO. This result is in disagreement with Appenz-eller et al. (1998), who suggested that western Greenland snow accumulation is a good proxy for the NAO index. In fact, Dethloff et al. (2002) have shown that the sim-ulated Greenland precipitation of HIRHAM4 agrees rather well with the reconstructed precipitation from Greenland ice cores (note that snow accumulation is nearly equal to precipitation over most of the ice sheet).

The combined effects of the NAO and increasing greenhouse gases and aerosols on Arctic precipitation are shown in Fig. 6b (HIRHAM4 simulations driven by the scenario simulation). As for the temperatures, there are also some remarkable accordances between the natural precipitation signal of the NAO and those under increasing greenhouse gases and aerosols. For example, the strong differences on the Pacific coast of North America are qualitatively very similar in both experi-ments. The same applies to the division of Greenland with respect to the NAO impact as well as for the higher precipitation over the eastern North Atlantic during the positive NAO phase. Nevertheless, there are also some differences, such as higher precipitation amounts over northern Europe during the negative phase in which the level of greenhouse gases and aerosols is enhanced as compared to the positive phase. This means that pre-cipitation over northern Europe is likely to be more strongly influenced by the changed atmospheric com-position than by the NAO. In addition, the precipitation signal over the Bering Strait, the Labrador Sea, and the southern Barents Sea is largely reversed as compared to the NAO only impact and could be associated with large changes of the sea-ice cover which occur within these sea regions in the course of the scenario simulation.

The precipitation changes between the years 2013–2020 and the years 2039–2046 are likewise statistically not significant, except for some local areas of eastern Siberia, Greenland, the Canadian Archipelago, and the Arctic Ocean in which the total precipitation amounts are partly very low. In consideration of the strong spa-tial as well as temporal variability of precipitation, a definite statement about the future precipitation evolu-tion is likely to be impossible, even if the future NAO changes would be known. Nevertheless, a modification of the precipitation distribution through the NAO is quite obvious in view of the large similarity of the pre-cipitation change patterns in both RCM experiments.

For comparison, the corresponding difference pat-terns of the GCM simulations are shown in Fig. 6c, d (note that the GCM data were interpolated to the HIRHAM4 grid, resulting in some odd spots). Both the control simulation and the scenario simulation show some general features obtained from the dynamical downscaling, but there are large deviations on smaller scales. These deviations are mostly linked to orographic anomalies due to the different horizontal resolutions, but occur as well over some parts of the ocean, e.g. the Greenland Sea, indicating differences in the reproduc-tion of cyclone tracks. Because cloud and precipitation processes in the RCM are only indirectly dependent on the boundary conditions, the RCM precipitation has a higher degree of freedom to respond to those internal model processes that are better reproduced due to higher horizontal resolution. Therefore, the RCM is not only able to provide spatial characteristics that are more de-tailed, but also to improve the magnitude of precipita-tion locally.

4.3 Synoptic variability of sea level pressure

As noted by Rinke and Dethloff (2000), the dependency on the lateral boundary forcing in a RCM for the Arctic is on the synoptic scale not as strong as in a corre-sponding model for mid-latitudes. Synoptic disturbances within the central Arctic region of HIRHAM4 are therefore more strongly determined by the internal physical processes of the model, from which many are dependent on the model resolution. To quantify syn-optic scale variability we have applied a digital filter that retains variability on a 2–6 day time scale to the simu-lated SLP data at each grid point for each winter. The standard deviations of the filtered SLP data then pro-vides a proxy for synoptic variability. This is a usual approach to identify synoptic disturbances (e.g. Hurrell and van Loon 1997; Osborn et al. 1999), but note that SLP variability in the 2–6 day window is not only originated by passing cyclones but also by anticyclonic activity.

Figure 7 shows the mean synoptic SLP variability (average over all winters) for the positive and negative NAO phases of both RCM experiments as well as for the driving GCM simulations. The positive phases (both CTRL + and SCEN +) are primarily characterized by a higher synoptic variability on the Pacific coast of North America and over the eastern North Atlantic where, in each case, the variability is also generally high. In the central Arctic and the Greenland region, SCEN + shows higher values than SCEN– (and any other period), whereas the synoptic variability in CTRL + is lower than in CTRL–. A further disagreement appears over the Eurasian continent and the Barents and Kara seas where the synoptic variability in CTRL– is slightly re-duced as compared to CTRL + and vice versa in the scenario periods.

Based on observational data, Serreze et al. (1997) have shown that more cyclones occur over the eastern North Atlantic in positive NAO phases (associated with a deeper Icelandic low), whereas cyclones in the areas of Labrador and the Barents and Kara seas are less fre-quent. However, over the past years, there was also a

(a) SLP synoptic variability: CTRL+

(b) SLP synoptic variability: CTRL−

(c) SLP synoptic variability: SCEN+

(d) SLP synoptic variability: SCEN−
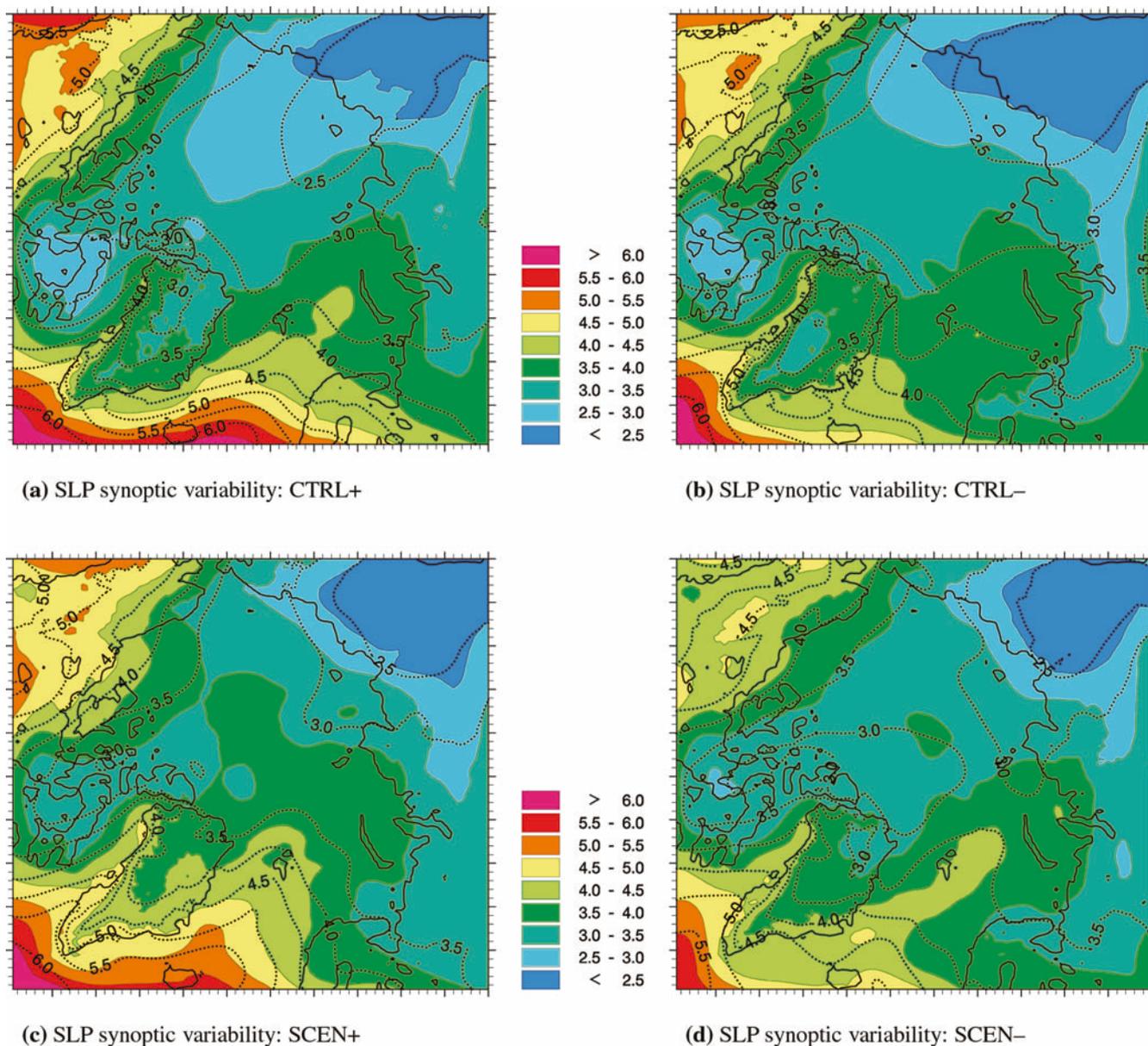
Fig. 7 Mean synoptic scale variability of sea level pressure (hPa) in winter (December–March) for the Arctic region: **a** CTRL+; **b** CTRL−; **c** SCEN+; **d** SCEN−. The simulation results of the RCM HIRHAM4 are shown by the *colour scale* and the results of the driving GCM simulations are shown by *dotted contours*. Coasts are represented by *solid contours*

general increase of cyclone events within these regions (see Serreze et al. 1997, Fig. 8) which cannot be attributed to the NAO. The first fact corresponds very well with the simulation results, because synoptic variability in the Icelandic low region is mainly caused by cyclones. The simulated differences between positive and negative phases in the areas of the Barents and Kara seas are rather low in both experiments, and a higher synoptic variability during negative phases emerges only in the scenario driven simulation of the RCM as noted before.

Compared to the driving GCM simulations, the RCM always generates a higher synoptic variability in the inner Arctic, particularly over the Barents and Kara seas where a high frequency of cyclones are also observed during winter (see Serreze et al. 1993, Fig. 2). This result indicates that overall, the RCM simulates more meridional cyclone tracks and/or a higher frequency of cyclogenesis within the inner Arctic. On the other hand, the variability in the RCM is lower along the southern and western coasts of Greenland. Kristjánsson and McInnes (1999) have demonstrated that the deepening of cyclones near Iceland is hampered by the presence of Greenland's orography. They conclude that models with an inadequate resolution of Greenland's orography may be expected to overestimate the strength of cyclones which pass through the area. Such biases, in turn, may impact the large-scale flow patterns over the North Atlantic and northern Europe. As shown

by Busch et al. (1999) for the North Atlantic and European region, the ECHAM GCM tends to overestimate the frequency of zonal weather patterns during winter and spring, which is likely to be associated with a more frequent zonal track of Atlantic cyclones. Altogether, the synoptic variability of the RCM appears to be closer to reality.

5 Summary and conclusions

Simulations of the Arctic winter climate have been performed with a high-resolution RCM, driven by a long-term control simulation and by a greenhouse gas and aerosol scenario simulation of two GCMs. These simulations have been applied to analyze the influence of the NAO on Arctic temperatures, precipitation, and synoptic SLP variability with simultaneous consideration of projected anthropogenic effects.

Both GCM simulations include a quite realistic interannual variability of the NAO with pronounced decadal regime changes, which are also occurring in a world with enhanced greenhouse gases and aerosols. The SLP differences between selected positive and negative NAO phases bear a great resemblance to the observed NAO pattern in both simulations, particularly over the Atlantic sector of the Northern Hemisphere. However over the North Pacific region, the normal pressure difference between positive and negative NAO phases appears to be modified by the changed atmospheric composition in the scenario simulation.

A statistically significant upward trend of the NAO index, as partly found in other model studies (e.g. Paeth et al. 1999), does not emerge in the scenario simulation using a simple local index. Indeed, there is a significant upward trend in the non-local AO index, but nevertheless this upward trend is not so well pronounced as in several other model studies (e.g. Ulbrich and Christoph 1999; Paeth et al. 1999; Fyfe et al. 1999; Shindell et al. 1999; Zorita and González-Rouco 2000). Furthermore, these model results disagree not only in terms of decadal fluctuations of the AO/NAO, but also in their simulated long-term trends. Even downward trends of the AO/NAO have been found in several scenario simulations of the HadCM2 model (Osborn et al. 1999; Zorita and González-Rouco 2000). Shindell et al. (1999) have argued that an AO/NAO trend emerges only in climate models that include a realistic representation of the stratosphere. A more realistic simulation of the stratospheric dynamics could then be very important for a realistic reproduction of AO/NAO regime changes. Although the ECHAM4 model used represents the stratosphere only very coarsely (five levels), it is also possible that the potential impacts of increasing greenhouse gases on the AO/NAO are decreased due to aerosols, because the temperature increase is also reduced as compared to a scenario simulation without involvement of aerosols.

As shown by Zorita and González-Rouco (2000), the trend of the AO/NAO is not only strongly dependent on the model, but also on the initial conditions of the simulations. If so, then changes in the frequency of AO/NAO regimes are likely to respond nonlinearly to small changes in the climate system, possibly not or not only caused by increasing greenhouse gases and aerosols. Consequently, the AO/NAO by itself may be of chaotic nature and rather unpredictable on decadal and longer time scales. From this point of view, the simulations may be considered only as an experiment for estimating the regional magnitude of NAO related climate changes in the Arctic and their relevance for the future climate evolution and not as a real climate prediction. The occurrence of a positive NAO phase at the beginning of the twentyfirst century and the subsequent change to the negative phase in the course of the scenario simulation used should accordingly be understood only as one of several possible realizations of the future climate evolution.

The simulation results of the RCM have shown a regionally significant influence of the NAO on winter temperatures and precipitation in some regions of the Arctic, especially over the northwestern Eurasian continent and parts of Greenland. For example, variations of mean winter temperatures of 3–6 K and mean winter precipitation of up to 100 mm occur over northern Europe and western Siberia as a result of regime changes of the NAO. However precisely there, precipitation responds even more to increasing greenhouse gases and aerosols than to the NAO, whereas in almost all other Arctic regions temperatures and precipitation are more strongly affected by the NAO. The temperature and precipitation changes are accompanied by changes in the synoptic SLP variability, particularly on the Pacific coast of North America and over the eastern North Atlantic where the variability is clearly higher during positive NAO phases.

The differences between the RCM and the driving GCM simulations are rather low with respect to near surface temperatures, but in terms of precipitation and synoptic SLP variability, the simulated patterns of the RCM are altogether more reliable than those of the GCM. However, in all model experiments, the Arctic climate is characterized by a spatial dichotomy concerning the NAO impact, expressed by antipodal effects in the western and eastern Arctic. This characteristic feature appears under enhanced greenhouse gases and aerosols as well. The magnitudes of temperature and precipitation changes associated with the NAO are in some regions clearly stronger than imaginable linear changes attributed to enhanced greenhouse gases and aerosols. Projected global changes of the atmospheric composition and internal circulation changes are thus competing with each other in their importance for the Arctic climate evolution in the near future.

It is not denied here that anthropogenic forcing will have no influence on either the frequency or the intensity of the NAO. Instead the view is advanced that the NAO is able to modulate future climate trends given the expected influence of anthropogenic effects. In view of the strong regional modification of Arctic temperatures and

precipitation due to regime changes of the NAO, the timing of a shift to another regime also plays a prominent role for a regional assessment of future Arctic climate changes. This conclusion may help to explain the large discrepancies of global climate models in projections of the future Arctic climate. A better understanding of the NAO with respect to its causes and possible feedbacks with other climate forcings seems to be an important step in order to enhance the reliability of Arctic climate projections.

References

Agnew T (1993) Simultaneous winter sea-ice and atmospheric circulation anomaly patterns. Atmos Ocean 31: 259–280

Ambaum MHP, Hoskins BJ, Stephenson DB (2001) Arctic Oscillation or North Atlantic Oscillation? J Clim 14: 3495–3507

Appenzeller C, Schwander J, Sommer S, Stocker TF (1998) The North Atlantic Oscillation and its imprint on precipitation and ice accumulation in Greenland. Geophys Res Lett 25: 1939–1942

Bromwich DH, Chen Q, Li Y, Cullather RI (1999) Precipitation over Greenland and its relation to the North Atlantic Oscillation. J Geophys Res 104: 22,103–22,115

Busch U, Dorn W, Roth R (1999) Study of upper winds in observations and ECHAM model simulations. Meteorol Z NF 8: 39–42

Chen B, Bromwich DH, Hines KM, Plan X (1995) Simulations of the 1979–1988 polar climates by global climate models. Ann Glaciol 21: 83–90

Christensen JH, Christensen OB, Lopez P, van Meijgaard E, Botzet M (1996) The HIRHAM4 regional atmospheric climate model. DMI Sci Rep 96-4, Danish Meteorological Institute, Copenhagen, Denmark

Corti S, Molteni F, Palmer TN (1999) Signature of recent climate change in frequencies of natural atmospheric circulation regimes. Nature 398: 799–802

Cubasch U, Meehl GA, Boer GJ, Stouffer RJ, Dix M, Noda A, Senior CA, Raper S, Yap KS (2001) Projections of future climate change. In: Houghton JT, Ding Y, Griggs DJ, Noguer M, van der Linden PJ, Dai X, Maskell K, Johnson CA (eds) Climate change 2001: The scientific basis. Contribution of Working Group I to the Third Assessment Report of the Intergovernmental Panel on Climate Change. Cambridge University Press, Cambridge, UK, pp 525–582

Curry JA, Rossow WB, Randall D, Schramm JL (1996) Overview of Arctic cloud and radiation characteristics. J Clim 9: 1731–1764

Dethloff K, Rinke A, Lehmann R, Christensen JH, Botzet M, Machenhauer B (1996) Regional climate model of the Arctic atmosphere. J Geophys Res 101: 23,401–23,422

Dethloff K, Weisheimer A, Rinke A, Handorf D, Kurgansky MV, Jansen W, Maaß P, Hupfer P (1998) Climate variability in a nonlinear atmosphere-like dynamical system. J Geophys Res 103: 25,957–25,966

Dethloff K, Schwager M, Christensen JH, Kiilsholm S, Rinke A, Dorn W, Jung-Rothenhäusler F, Fischer H, Kipfstuhl S, Miller H (2002) Recent Greenland accumulation estimated from regional climate model simulations and ice core analysis. J Clim 15: 2821–2832

Dorn W, Dethloff K, Rinke A, Botzet M (2000) Distinct circulation states of the Arctic atmosphere induced by natural climate variability. J Geophys Res 105: 29,659–29,668

Folland CK, Karl TR, Christy JR, Clarke RA, Gruza GV, Jouzel J, Mann ME, Oerlemans J, Salinger MJ, Wang SW (2001) Observed climate variability and change. In: Houghton JT, Ding Y, Griggs DJ, Noguer M, van der Linden PJ, Dai X, Maskell K, Johnson CA (eds) Climate change 2001: The scientific basis. Contribution of Working Group I to the Third Assessment Report of the Intergovernmental Panel on Climate Change. Cambridge University Press, Cambridge, UK, pp 99–181

Fyfe JC, Boer GJ, Flato GM (1999) The Arctic and Antarctic Oscillations and their projected changes under global warming. Geophys Res Lett 26: 1601–1604

Giorgi F, Marinucci MR (1996) An investigation of the sensitivity of simulated precipitation to model resolution and its implications for climate studies. Mon Weather Rev 124: 148–166

Gustafsson N (1993) HIRLAM2 final report. HIRLAM Tech Rep 9, Swedish Meteorological and Hydrological Institute, Norrköping, Sweden

Handorf D, Petoukhov VK, Dethloff K, Eliseev AV, Weisheimer A, Mokhov II (1999) Decadal climate variability in a coupled atmosphere–ocean climate model of moderate complexity. J Geophys Res 104: 27,253–27,275

Hansen J et al (1997) Forcings and chaos in interannual to decadal climate change. J Geophys Res 102: 25,679–25,720

Haywood JM, Stouffer RJ, Wetherald RT, Manabe S, Ramaswamy V (1997) Transient response of a coupled model to estimated changes in greenhouse gas and sulfate concentrations. Geophys Res Lett 24: 1335–1338

Houghton JT, Callendar BA, Varney SK (eds) (1992) Climate change 1992: the supplementary report to the IPCC scientific assessment. Cambridge University Press, Cambridge, UK

Hurrell JW (1995) Decadal trends in the North Atlantic Oscillation: regional temperatures and precipitation. Science 269: 676–679

Hurrell JW, van Loon H (1997) Decadal variations in climate associated with the North Atlantic Oscillation. Clim Change 36: 301–326

Kerr RA (1999) A new force in high-latitude climate. Science 284: 241–242

Kristjánsson JE, McInnes H (1999) The impact of Greenland on cyclone evolution in the North Atlantic. Q J R Meteorol Soc 125: 2819–2834

Legutke S, Voss R (1999) The Hamburg atmosphere–ocean coupled circulation model ECHO-G. DKRZ Tech Rep 18, Dtsch Klimarechenz, Hamburg, Germany

Lynch AH, Chapman WL, Walsh JE, Weller G (1995) Development of a regional climate model of the western Arctic. J Clim 8: 1555–1570

Noguer M, Jones R, Murphy J (1998) Sources of systematic errors in the climatology of a regional climate model over Europe. Clim Dyn 14: 691–712

Oberhuber JM (1993a) Simulation of the Atlantic circulation with a coupled sea ice-mixed layer-isopycnal general circulation model. Part I: model description. J Phys Oceanogr 23: 808–829

Oberhuber JM (1993b) The OPYC ocean general circulation model. DKRZ Tech Rep 7, Dtsch Klimarechenz, Hamburg, Germany

Osborn TJ, Briffa KR, Tett SFB, Jones PD, Trigo RM (1999) Evaluation of the North Atlantic Oscillation as simulated by a coupled climate model. Clim Dyn 15: 685–702

Paeth H, Hense A, Glowienka-Hense R, Voss R, Cubasch U (1999) The North Atlantic Oscillation as an indicator for greenhouse-gas induced regional climate change. Clim Dyn 15: 953–960

Palmer TN (1999) A nonlinear dynamical perspective on climate prediction. J Clim 12: 575–591

Rinke A, Dethloff K (2000) On the sensitivity of a regional Arctic climate model to initial and boundary conditions. Clim Res 14: 101–113

Rinke A, Dethloff K, Christensen JH, Botzet M, Machenhauer B (1997) Simulation and validation of Arctic radiation and clouds in a regional climate model. J Geophys Res 102: 29,833–29,847

Roeckner E, Arpe K, Bengtsson L, Christoph M, Claussen M, Dümenil L, Esch M, Giorgetta M, Schlese U, Schulzweida U (1996) The atmospheric general circulation model ECHAM-4: Model description and simulation of present-day climate. MPI Rep 218, Max Planck Institute for Meteorology, Hamburg, Germany

Roeckner E, Bengtsson L, Feichter J, Lelieveld J, Rodhe H (1999) Transient climate change simulations with a coupled atmosphere–ocean GCM including the tropospheric sulfur cycle. J Clim 12: 3004–3032

Serreze MC, Box JE, Barry RG, Walsh JE (1993) Characteristics of Arctic synoptic activity, 1952–1989. Meteorol Atmos Phys 51: 147–164

Serreze MC, Carse F, Barry RG, Rogers JC (1997) Icelandic low cyclone activity: Climatological features, linkages with the NAO, and relationships with recent changes in the Northern Hemisphere circulation. J Clim 10: 453–464

Shindell DT, Miller RL, Schmidt GA, Pandolfo L (1999) Simulation of recent northern winter climate trends by greenhouse-gas forcing. Nature 399: 452–455

Stouffer RJ, Manabe S (1999) Response of a coupled ocean–atmosphere model to increasing atmospheric carbon dioxide: sensitivity to the rate of increase. J Clim 12: 2224–2237

Tao X, Walsh JE, Chapman WL (1996) An assessment of global climate model simulations of Arctic air temperatures. J Clim 9: 1060–1076

Thompson DWJ, Wallace JM (1998) The Arctic Oscillation signature in the wintertime geopotential height and temperature fields. Geophys Res Lett 25: 1297–1300

Ulbrich U, Christoph M (1999) A shift of the NAO and increasing storm track activity over Europe due to anthropogenic greenhouse gas forcing. Clim Dyn 15: 551–559

Voss R, Mikolajewicz U (2001) Long-term climate changes due to increased CO_2 concentration in the coupled atmosphere–ocean general circulation model ECHAM3/LSG. Clim Dyn 17: 45–60

Wallace JM (2000) North Atlantic Oscillation/annular mode: two paradigms – one phenomenon. Q J R Meteorol Soc 126: 791–805

Wolff JO, Maier-Reimer E, Legutke S (1997) The Hamburg ocean primitive equation model. DKRZ Tech Rep 13, Dtsch Klimarechenz, Hamburg, Germany

Zorita E, González-Rouco F (2000) Disagreement between predictions of the future behavior of the Arctic Oscillation as simulated in two different climate models: implications for global warming. Geophys Res Lett 27: 1755–1758